BOR DERGİSİ
JOURNAL OF BORON
https://dergipark.org.tr/boron

Influence of boron bearing fillers on flame retardancy properties of huntite hydromagnesite filled ductile PLA biocomposites

Aysegul Erdem[1,*], **Mehmet Dogan**[2]

[1]*Erciyes University, Department of Textile Engineering, Kayseri, 38039, Turkiye*

ARTICLE INFO

Article history:
Received June 25, 2022
Accepted February 23, 2023
Available online March 31, 2023

Research Article

DOI: 10.30728/boron.1135702

Keywords:
Boron oxide
Colemanite
Flammability
Huntite hydromagnesite
Polylactic acid

ABSTRACT

In this work, the flame retardancy influences of colemanite and boron oxide are investigated n huntite-hydromagnesite (HH) containing plasticized poly (lactic acid) (PLA) biocomposites. The composites are characterized using limiting oxygen index (LOI), horizontal (UL 94 HB) and vertical (UL-94 V) burning tests, mass loss calorimeter (MLC), and thermogravimetric analysis (TGA). The addition of colemanite causes enhanced fire retardancy performance with higher UL-94 V rating and LOI value and lower peak heat release rate (pHRR) value. V0 rating and the highest LOI value are observed with the addition 1 wt% colemanite. The samples get V1 rating for the loading amount of 3 and 5 wt% colemanite. When the concentration of colemanite reaches to 5 wt%, pHRR and average heat release rate (avHRR) values are lower than those of the reference sample. Addition of boron oxide causes improvement in LOI value. The highest LOI value (33.2) is observed in 5 and 10 wt% boron oxide containing samples.

1. Introduction

Boron-based agents are employed as multifunctional flame retardant fillers either used alone or in conjunction with the other flame retardants for their adjuvant effect in various polymeric materials. Boron-based additives interact synergistically with various fillers containing metal, phosphorus, nitrogen, and halogen atoms [1-6]. Different boron compounds such as zinc borate ($B_2O_6Zn_3$) [7-12], boroxo siloxanes [13], and boric acid (H_3BO_3) [14] are used in different polymers as synergistic additives with commercially important mineral fillers, such as aluminum trihydroxide ($Al(OH)_3$, ATH) [7-11], and magnesium hydroxide ($Mg(OH)_2$, MH) [9, 10, 13, 14] in different polymers.

Huntite & hydromagnesite ($(Mg_3Ca(CO_3)_4$ & $Mg_5(CO_3)_4(OH)_2.4H_2O$, HH)), a carbonate-based mineral mixture that occurs naturally, is employed as a functional additive in various polymers. Fire retardant behavior of HH is almost similar to ATH and MH. HH has higher potential for wide application than ATH due to the higher onset decomposition temperature (220-240 °C). In contrast to ATH (1300 Jg^{-1}), HH has a lower enthalpy of decomposition (990 Jg^{-1}) [15-17]. Thus, the flame retardancy action of HH is enhanced with synergic action studies employing red phosphorus [18], expandable graphite [19], zinc borate [20, 21], antimony trioxide (Sb_2O_3) [22-24], and boric acid [22].

The flame retardant performance of HH was assessed in polylactic acid (PLA) [25] in our previous study. It was found in these studies that 60 wt% and 70 wt% HH were needed for obtaining V0 rating in vertical UL-94 test (UL-94 V). The addition of such high filler loading causes detrimental effect on mechanical poperties. With synergistic effect studies, higher flame retardant performance can be achieved with using same amount of additive. Accordingly, less flame retardant additive can be used for achieving same retardant performance.

Colemanite (Col), a naturally occurring boron mineral, is a promising flame retardant additive in plastics. It was employed as a primary flame retardant agent in epoxy resin [26], biocomposite applications [27-29], and ethylene vinyl acetate [30]. It was also employed as a synergistic additive with brominated flame retardant [31], intumescent based flame retardant [32] and ATH [33, 34]. Cavodeau et al. analyzed the synergistic action of colemanite with ATH and MH in polyethylene based copolymers. It was found that no synergistic effect was observed and it acted as an efficient smoke suppressant [33]. Isıtman et al. examined the synergistic performance between ATH and colemanite in polyethylene. The highest synergistic interaction was obtained with the addition of 10 wt% colemanite instead of ATH [34].

*Corresponding author: aysgulerdem@gmail.com

Boron oxide (B_2O_3) is industrially used in the production of numerous glass-based materials, ceramics and enamels, detergents, and soaps. In literature, it was also utilized as a flame-retardant filler for polymers, either by itself or in combination with other functional fillers [26, 35-38]. Ibibikcan and Kaynak investigated the synergistic interaction between B_2O_3 and ATH in polyethylene based cable sheathing material. The highest synergistic interaction was achieved with the addition of 10 wt% B_2O_3 instead of ATH [38].

The motivation of this work is to enhance the flame retardancy performance of HH using colemanite and B_2O_3 as synergistic additives in plasticized PLA composites. As our best knowledge, there is no study investigating the synergistic interaction between HH and boron compounds (Col and B_2O_3) in any polymeric material is found in literature. In this study, composite materials were produced with extrusion process and the extrudates were further shaped by injection moulding and compression moulding for flammability tests. The fire retardant performance of the samples was characterized by limiting oxygen index (LOI), horizontal UL-94 test, (UL-94 HB), UL-94 V and mass loss calorimeter (MLC) test.

2. Experimental Works

2.1. Materials

PLA (MFI (22 g/10 min (210°C, 2.16 kg)), 1.24 g/cm^3) was purchased from Nature Works with the commercial name of Ingeo TM Biopolymer 3001D. Ultracarb LH3 (a natural huntite hydromagnesite mixed mineral) was purchased from Likya Minelco, Türkiye. It has the particle sizes of d_{98}:<10 µm, d_{90}:4-6 µm, d_{50}:1-2 µm and the density of 2.4 g/cm^3. Silane coupling agent (3-glycidoxy propyl trimethoxy silane), acetone and the plasticizer (acetyl tri butyl citrate) were purchased from Sigma Aldrich. B_2O_3 and Col were obtained from ETİ Maden, Türkiye. B_2O_3 has the specific weight and molecular weight of 2.17 g/cm^3 and 69.62 g/mol, respectively. Col (411.08 g/mol) has the density of 2.6 g/cm^3.

2.2. Silane Treatment of HH

3-glycidoxy propyl trimethoxy silane was used as a silane coupling agent since the best mechanical properties were obtained by it, in our previous study [25]. Silane coupling agent was diluted with acetone in order to cover the HH surface evenly. Silane coupling agent was used as 5 wt% of HH. The resulting mixture was constantly stirred after HH was added. The acetone was evaporated at 80°C overnight in oven. The characterization of modified HH was given in our previous 111 study [25].

2.3. Composite Production

Before the extrusion process, PLA and the flame retardant additives were desiccated in an oven at 80°C for 24h. The compounding process was performed with the temperature profile of 160-165-170-165-40°C at 100 rpm using a twin screw extruder (Gülnar Makine, Türkiye). After the extrusion process, the samples were shaped using injection-molding machine (Xplore 12 ml Micro-Injection Molding Machine, Netherlands) at 190°C. Samples for MLC test were molded using electrically heated hydrolytic hot-press (Gülnar Makine, Türkiye) at 170°C for 3 min. All formulations contain constant amount of plasticizer (P, 12 wt%). The added amount of plasticizer was removed from PLA content. The synergistic interaction was studied under constant filler amount of 60 wt% and the added boron compounds were deducted from the HH amount. In sample nomenclature, the abbreviations PLA, P, HH, Col, B_2O_3 are used for poly (lactic acid), plasticizer (acetyl tributyl citrate), huntite-hydromagnesite, colemanite and boron oxide, respectively. The sample coded as PLA/ 12P/ 57 HH/ 3Col refers to the composites containing 12 wt% plasticizer, 57 wt% HH and 3 wt% Col, respectively.

2.4. Characterization Methods

Thermogravimetric analysis (TGA) (Hitachi-High Tech STA-7300) tests were performed from 30°C to 800°C with a rate of 10°C/min under inert N_2 flow. The flammability characteristics of the samples were analyzed with limiting oxygen index (LOI, Fire Testing Technology (FTT)), Underwriters Laboratories horizontal burning (UL94 HB) and Underwriters Laboratories vertical burning (UL 94 V) tests according to ASTM D2863, ASTM D635, and ASTM D3801, respectively. Samples dimensions for LOI and UL-94 tests were (130×6.5×3.2 mm^3) and (130×13×3.2 mm^3), respectively. Mass loss calorimeter (MLC) (FTT, U.K) tests were performed at an external heat flux of 35 kW/m^2 according to the ISO 13927. The residues obtained after MLC test were analyzed using scanning electron microscopy (SEM, Zeiss GEMINI 500), attenuated total reflection Fourier transform infrared (ATR-FTIR, Bruker Optics IFS 66/S series FT-IR spectrometer) at 4000-400 cm^{-1} with 32 scans, and X-ray diffraction analysis (XRD, Rigaku SmartLab) at a scan rate of 1°/min over the range of 2Θ=10°-90°. Before SEM analysis, the residues were sputter-coated with gold to ensure the conductivity.

3. Results and Discussions

3.1. Thermal Decomposition of the Additives

TThermal decomposition characteristics of the flame retardant additives (HH, Col and B_2O_3) were examined via TGA analysis. TGA and DTG curves of the additives were given in Figure 1. Table 1 includes the pertinent data. HH undergoes endothermic decomposition in four steps with the loss of H_2O and CO_2. In the first degradation step, the loss of crystal water occurs from hydromagnesite structure. In other degradation steps, the CO_2 generation occurs from HH structure. MgO and CaO based inorganic residues are formed at the end of the decomposition steps [15, 16]. Col

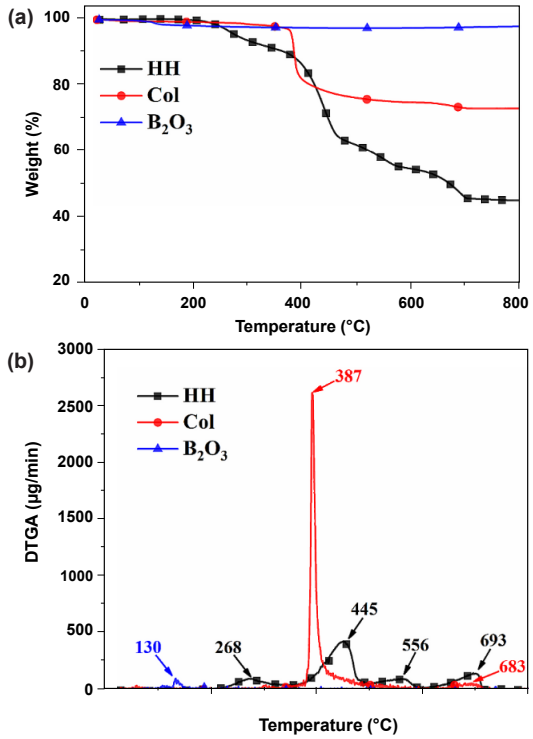

Figure 1. a) TGA and b) DTGA curves of the additives.

Table 1. TGA data of the additives and composites.

SAMPLE	$T_{5\%}$ (ºC)[a]	T_{max1} (ºC)[b]	T_{max2} (ºC)[b]	T_{max3} (ºC)[b]	T_{max4} (ºC)[b]	Char yield (%)[c]
HH	285	267	445	556	694	45.2
Col	390	387	-	-	-	73.3
B_2O_3	-	130	-	-	-	98.2
PLA/12P/60HH	228	251	340	435	675	28.8
PLA/12P/59HH/1Col	227	250	333	417	672	29.4
PLA/12P/57 HH/3Col	217	252	334	414	671	31.2
PLA/12P/55 HH/5Col	221	252	334	413	671	31.4
PLA/12P/50 HH/10Col	220	252	331	407	671	32.2
PLA/12P/59HH/1B_2O_3	207	252	337	422	650	32.1
PLA/12P/57HH/3B_2O_3	220	246	329	419	650	31.4
PLA/12P/55HH/5B_2O_3	217	243	330	413	652	34.9
PLA/12P/50 HH/10B_2O_3	211	243	327	415	648	36.4

a:Temperature at 5% weight loss b: The maximum degradation rate temperature c: CharYield at 800ºC.

decomposes in two steps via dehydration and dehydroxylation at 387°C and 683°C with leaving 73.3% inorganic residue based on calcium borate $Ca_3(BO_3)_2$ [33, 39]. A small decomposition peak was seen at 130°C owing to the loss of physically absorbed water during the decomposition of B_2O_3. It retains 98.2 % of its weight. The degradation routes of the additives are given below;

$Mg_5(CO_3)_4(OH)_2.4H_2O \longrightarrow 5MgO + 4CO_2 + 5H_2O$ (200-450°C) (1)
(Hydromagnesite)

$Mg_3Ca(CO_3)_4 \longrightarrow 3MgO + CaO + 4CO_2$ (450-800°C) (2)
(Huntite)

$2Ca[B_3O_4(OH)_3]H_2O \longrightarrow Ca_2B_6O_{11} + 5H_2O$ (390°C) (3)
(Colemanite)

$B_2O_3 \longrightarrow B_2O_3 + H_2O$ (130°C) (4)
(Boron oxide) (H_2O: physically absorbed water)

3.2. Thermal Decomposition of the Composites

Thermal decomposition behaviors of the samples were examined via TGA test. TGA and DTG curves of the samples are given in Figure 2. Table 1 includes the pertinent data. The addition of boron compounds decreased the initial thermal stability ($T_{5\%}$). All samples degraded in four successive decomposition steps. In the initial step, the degradation of PLA and hydromagnesite occured simultaneously. The other steps arose from additive decompositions.

With the addition of Col, the first and fourth step degradation temperatures did not change whereas the second and third step degradation temperatures decreased. With the addition of B_2O_3, degradation temperatures of all steps reduced distinctly. The observed trend was thought to be the formation of boric acid during the decomposition. The formed boric acid interacts with compounds (hydromagnesite, huntite, calcium carbonate) present in the HH. It is known from literature that some part of the Col can be converted into boric acid in aqueous acidic medium [40, 41]. In the presence of acidic degradation products of PLA (acrylic acid, lactol lactic acid and acetic acid) [42, 43] and water, the minor amount of boric acid can form. It is also known that B_2O_3 is converted into boric acid in the presence of water [2]. Some part of B_2O_3 is converted to boric acid when it interacts with water released from hydromagnesite structure. This conversion occurs more readily than Col. Thus, the reduction in degradation temperatures becomes prominent in the case of B_2O_3. The addition of boron compounds causes high residue yield since they retain their weight higher than HH during the decomposition. The addition of 10 wt% B_2O_3, which keeps its 98.2 wt%, results in the maximum residue yield (36.4%).

3.3. Mass Loss Calorimeter Studies

MLC studies are commonly applied to examine the fire retardancy behavior of the polymer based composites. The heat release rate (HRR) versus time curves of the composites are seen in Figure 3. Table 2 includes pertinent data. The digital and SEM images of residues are depicted in Figures 4 and 5. In B_2O_3 containing composites, the decreasing trend in time to ignition (TTI) values is observed. As observed in TGA section, the initial thermal stability of the B_2O_3 bearing composites is much lower than reference sample. Thus, the required amounts of combustible products for ignition reach in shorter time than the reference samples.

The reference sample (PLA/12P/60HH) had pHRR, avHRR and THE values of 172 kW/m^2, 107 kW/m^2 and 30 MJ/m^{2}g, respectively. pHRR and avHRR values reduce steadily as the Col amount increases. When the concentration of Col reached to 5 wt%, pHRR and avHRR values were lower than those of the reference sample. The pHRR and avHRR values reduced at about 15% and 8% with the addition of 10 wt% Col, respectively. As seen from Figure 4, addition

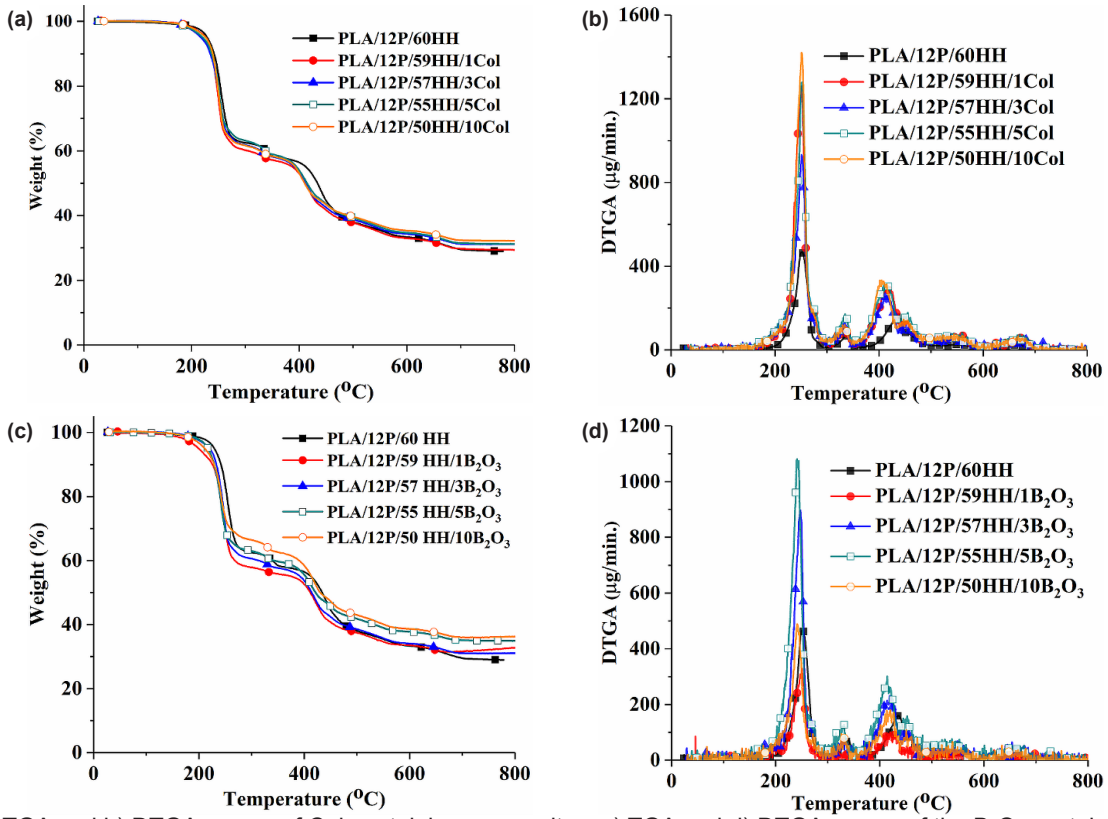

Figure 2. TGA and b) DTGA curves of Col containing composites, c) TGA and d) DTGA curves of the B_2O_3 containing composites.

of Col caused the formation compact residue with less cracks with increasing amount because of its sintering effect. Thus, the decrease in pHRR was attributed to the enhancement in the protective function of char structure. All B_2O_3 containing composites had higher pHRR and avHRR values than the reference sample. During the test, the samples cracked just after the ignition and segregated residue formation occurs (Figure 5). It is known that the cracks ave detrimental effect on the protective function of the residue. Accordingly, the higher pHRR and avHRR values were seen in all B_2O_3 containing samples. However, pHRR and avHRR values reduced with increasing B_2O_3 content. As seen in SEM images, segregated parts had compact structure. In 5 and 10 wt% B_2O_3 containing samples, no cracks and holes were observed since B_2O_3 has ability to form vitreous structure with sintering effect.

Boron-bearing composites retained more residue than the reference sample. The residue yield increases as boron compound amount rises. It was understood from FTIR studies that the residue yield rise stems mainly from that the undecomposed portion of boron compounds rather than in complete pyrolysis. The FTIR spectra of the char residues are depicted in Figure 6. After the combustion process, only HH containing composite had characteristic peaks seen at 3700, 2980, 2890, 1420, 1060 and 880 cm^{-1}. The peak seen at 3700 cm^{-1} was attributed to OH stretching vibration. The peaks seen at 1420, 1060 and 880 cm^{-1} were caused by the asymmetric and symmetric stretching vibrations of carbonate group present in the

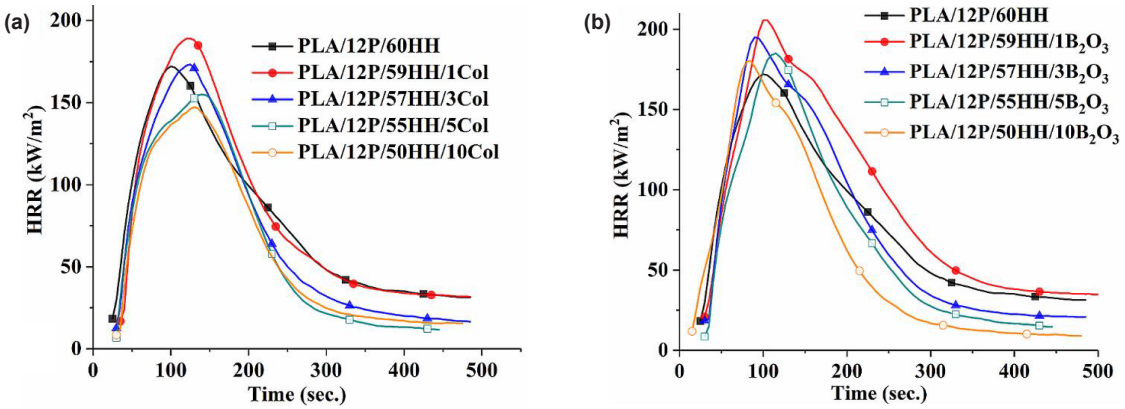

Figure 3. HRR curves of a) Col containing composites, b) B_2O_3 containing composites.

Table 2. MLC data of the composites.

SAMPLE	TTI (sec)	pHHR ($kW.m^{-2}$)	AvHRR ($kW.m^{-2}$)	pMLR (gs^{-1})	THE (MJ/m^2)	THE/TML (MJ/m^2g)	Residue (%)
PLA/12P/60HH	28	172 ± 12	107±9	0.18	30 ± 2	1.53	40.2
PLA/12P/59HH/1Col	37	189 ± 9	119 ± 8	0.17	30 ± 2	1.54	40.8
PLA/12P/57 HH/3Col	29	173 ± 11	106 ± 8	0.14	29 ± 1	1.59	42.4
PLA/12P/55 HH/5Col	28	155 ± 13	100 ± 7	0.19	28 ± 2	1.48	43.7
PLA/12P/50 HH/10Col	33	147 ± 14	98 ± 9	0.16	28 ± 2	1.50	44.6
PLA/12P/59HH/1B_2O_3	30	206 ± 16	117 ± 12	0.18	31 ±3	1.52	41.3
PLA/12P/57HH/3B_2O_3	33	195 ± 15	123 ± 13	0.17	30 ± 3	1.46	42.8
PLA/12P/55HH/5B_2O_3	22	185 ± 12	113 ± 14	0.17	29 ± 2	1.53	44.1
PLA/12P/50 HH/10B_2O_3	18	180 ± 13	108 ± 9	0.16	29 ± 2	1.54	45.9

HH structure [18-20]. With the addition of boron compounds, only difference was observed at 1250 cm^{-1} seen as a shoulder due to the asymmetric stretching vibrations of B-O group. The other characteristic peaks of boron compounds (around 1000 cm^{-1} (B-O symmetric vibrations)), around 750 cm^{-1} (B-O-B bending vibration) masks with the characteristic peaks of HH [44]. Small peaks were observed at 2980 and 2890 cm^{-1} due to the aliphatic chain structure found in the residue. Insignificant change was seen in the intensity of these peaks with the use of boron compounds. Accordingly, no prominent difference was observed in total heat evolved (THE) values since almost complete pyrolysis occurred. Total heat evolved to total mass loss ratios (THE/TML) of the sample were almost the same and lies between 1.46 and 1.59. This finding

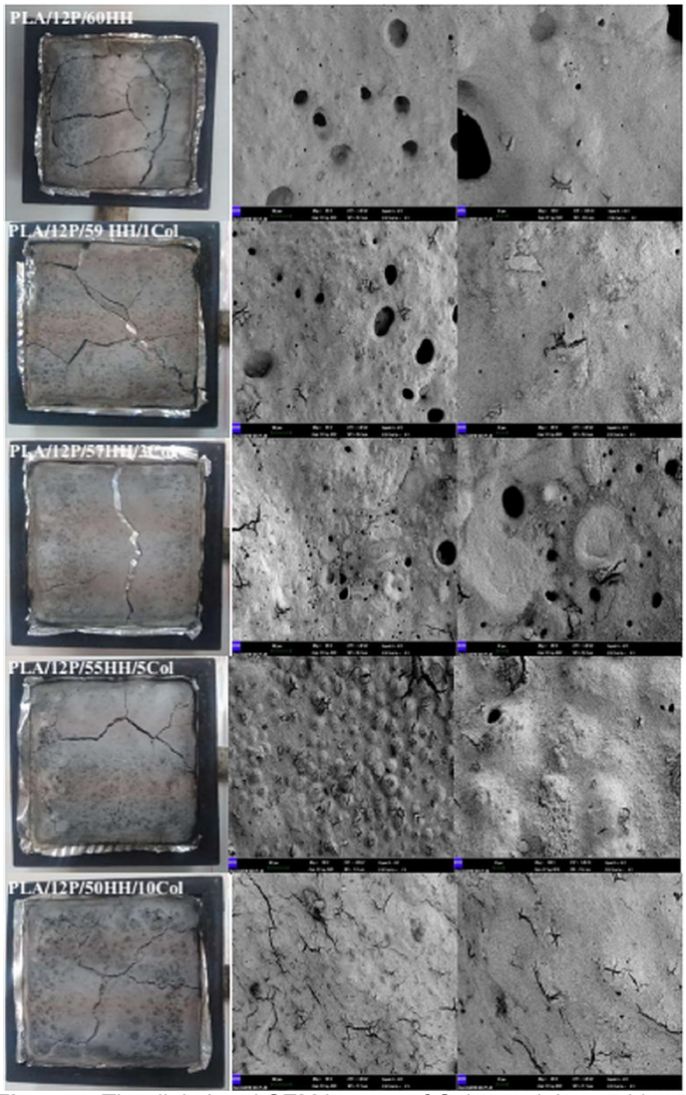

Figure 4. The digital and SEM images of Col containing residues.

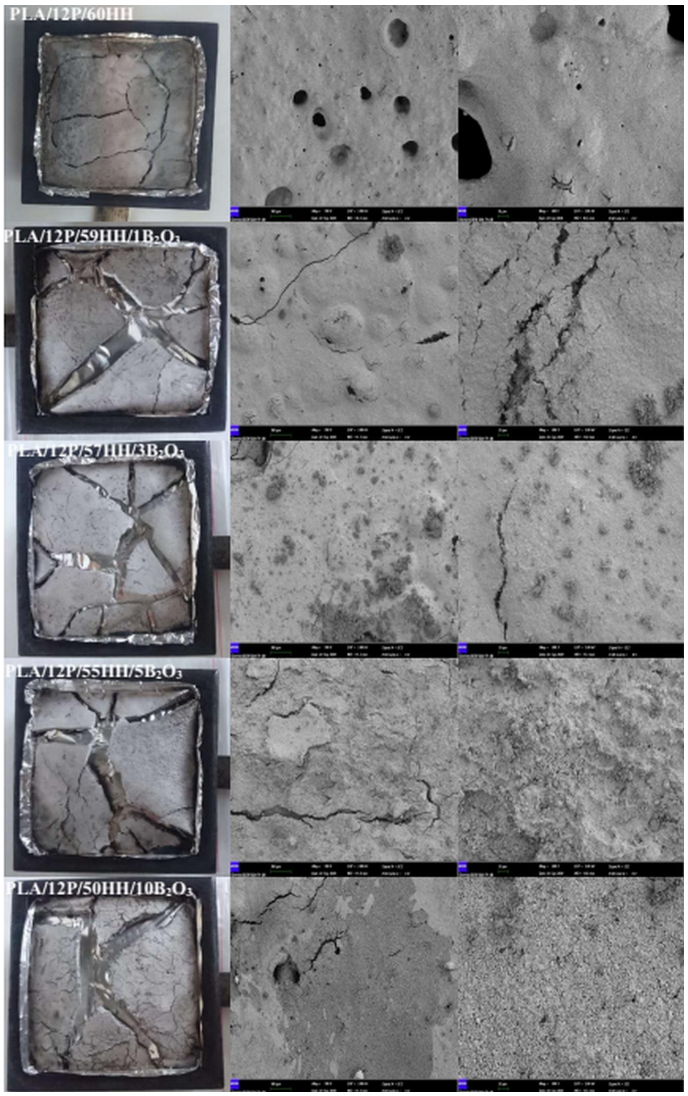

Figure 5. The digital and SEM images of B_2O_3 containing residues.

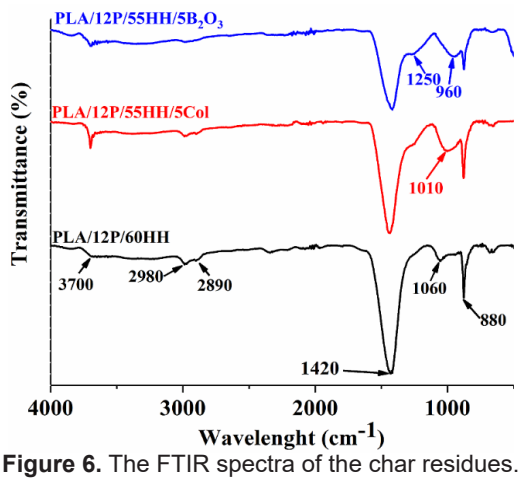

Figure 6. The FTIR spectra of the char residues.

clearly shows that Col and B_2O_3 exerted their synergistic effect in the condensed phase in contrast to in the gas phase.

In order to understand the interaction between HH and boron compounds, XRD analyses were performed to fillers heated at 500°C for 15 minutes and the residues remained after MLC test. The related results are shown in Figure 7. As seen from Figure 7, HH had characteristics peaks labelled with 1, 2, 3 corresponding to $CaMg(CO_3)_2$, (JCPDS card no 11-78), CaO (JCPDS card no: 37-1497), MgO (JCPDS card no 78-0430), respectively [18]. The residue of pure HH containing sample showed similar peaks. With the addition of Col, no meaningful change was observed in XRD results. With the addition of B_2O_3, the intensity of peak labelled with 1 (huntite) reduced, and the intensity of peaks labelled with 2 (CaO) and 3 (MgO) increased. It was concluded that the presence of B_2O_3 favors the degradation of huntite. As stated in TGA section in details, the presence of B_2O_3 reduced the degradation temperature of huntite due to acid-base interaction.

3.4. Flammability Properties

The fire retardancy performance of the samples are evaluated by LOI, UL-94 V and UL-94 HB tests. The pertinent data are seen in Table 3. The reference sample had the LOI value and UL-94 V rating of 29.8% and V2, respectively. During the UL-94 V test, a large burning piece of reference sample dropped and the sample

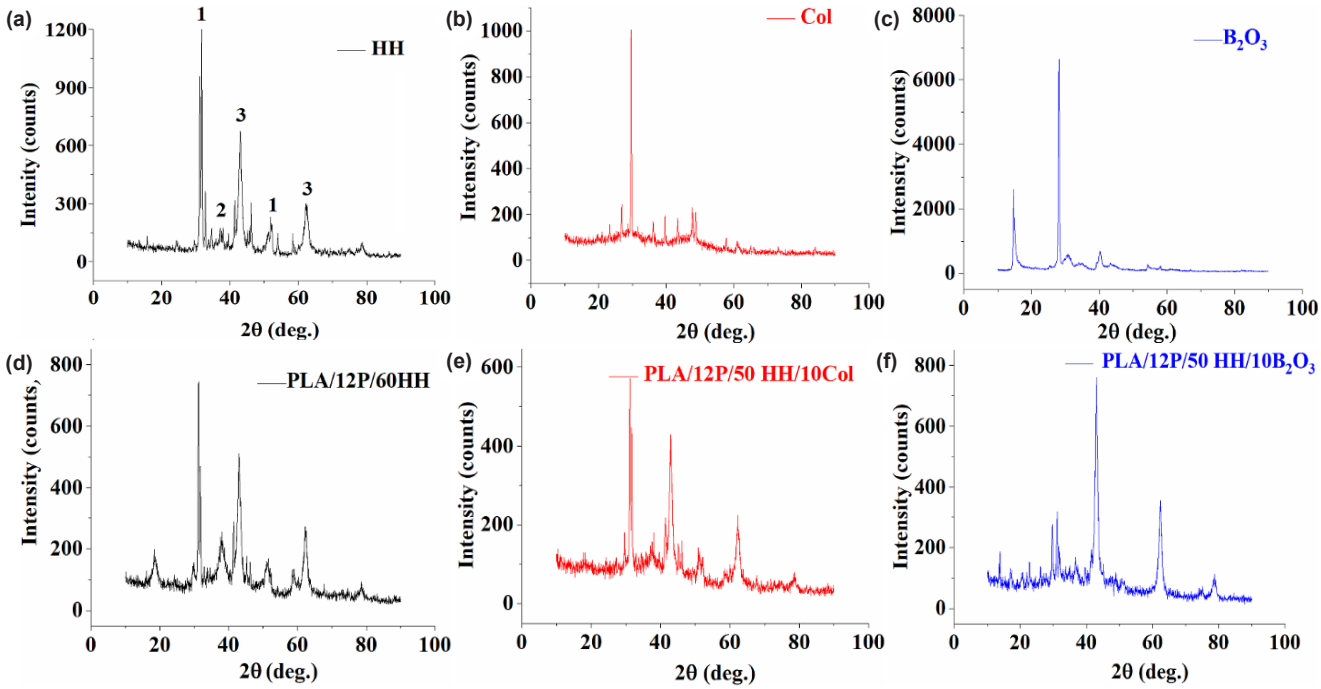

Figure 7. XRD graphs of the fillers heat at 500ºC for 15 minutes and the residues remained after MLC test.

extinguished just after dripping. It was thought that dripping stems from the presence of plasticizer in such high mineral filler loading of 60 wt%. The presence of plasticizer reduced the melt viscosity with reduced interchain interactions and increased the free volume [45-47]. All samples burned out prior to the flame coming to the initial mark in UL-94 HB test.

A addition of Col altered the UL-94 V rating via ceasing the dripping [48]. The maximum UL-94 rating V0 was obtained with the addition of 1 wt% Col. The samples got V1 rating in the loading amount of 3 and 5 wt% Col. Maximum LOI value was achieved with addition of 1 wt%. With increasing amount of Col, LOI value reduced steadily. When the Col concentration became 10 wt%, LOI value was lower than the reference sample. On contrary to Col, B_2O_3 addition did not cease dripping. Thus, all B_2O_3 samples got V2 rating. B_2O_3 admixture raised the LOI value and the highest LOI value was observed for 5 and 10 wt% B_2O_3 containing samples.

Table 3. Flammability characteristics of the composites.

SAMPLE	UL-94 V	UL94 HB		LOI
		t/sn	L/mm	
PLA/12P/60HH	V2	-	-	29.8
PLA/12P/59HH/1Col	V0	-	-	32.5
PLA/12P/57 HH/3Col	V1	-	-	31.0
PLA/12P/55 HH/5Col	V1	-	-	30.5
PLA/12P/50 HH/10Col	V2	-	-	28.3
PLA/12P/59HH/1B_2O_3	V2	-	-	32.3
PLA/12P/57HH/3B_2O_3	V2	-	-	32.3
PLA/12P/55HH/5B_2O_3	V2	-	-	33.6
PLA/12P/50 HH/10B_2O_3	V2	-	-	33.6

4. Conclusion

In this study, effect of Col and B_2O_3 on the thermal and flammability behaviors of HH containing plasticized PLA based composites was investigated. TGA, LOI, UL-94 V, UL-94 HB and MLC were used to characterize the composites. According to the TGA results, the presence of boron compounds reduced the initial thermal stability of the composites and favored the residue yield with increasing amount. The adjuvant effect of Col and B_2O_3 was seen on the fire retardant properties of the composites. Addition of Col caused enhancement in UL-94 V rating and LOI value and reduction in pHRR value. The pHRR value reduced at about 15% with the addition of 10 wt% Col. Addition of Col improved protective function of char structure with increasing amount because of its sintering effect. The addition of B_2O_3 caused an improvement only in LOI value. The highest LOI value (33.2) was observed for 5 and 10 wt% B_2O_3 containing composites.

Acknowledgements

This study is supported by TUBITAK under the project number of 118M203. Aysegul Erdem gets scholarship from Council of Higher Education in the scope of doctorate program of YOK 100/2000.

References

[1] Shen, K. K. (2014). Non-halogenated flame retardant handbook. In A. B. Morgan (Ed.). Boron-Based *Flame Retardants in Non-Halogen-Based Polymers* (pp.201-241). Scrivener Publishing LLC. ISBN 978-1-118-68624-9.

[2] Shen, K. K. (2009). Fire retardancy of polymeric materials. In C. A. Wilkie & Morgan A. B. (Eds.). *Boron Based Flame Retardants and Flame Retardancy* (pp.309-336).

CRC Press. ISBN 978-1-119-75056-7.

[3] Shen, K.K. (2014). Polymer green flame retardants. In C. D. Papaspyrides & P. Kiliaris (Eds.). *Review of Recent Advances on The Use of Boron-Based Flame Retardants*. (pp. 367-388). Elsevier. ISBN 978-0-444-53808-6.

[4] Shen, K. K., Kochesfahani, S., & Jouffret, F. (2008). Zinc borates as multifunctional polymer additives. *Polymers for Advanced Technologies*, *19*(6), 469-474.

[5] Bourbigot, S., Le Bras, M., Leeuwendal, R., Shen, K. K., & Schubert, D. (1999). Recent advances in the use of zinc borates in flame retardancy of EVA. *Polymer Degradation and Stability*, *64*, 419-425.

[6] Dogan, M, Dogan, S. D., Savas, L. A., Ozcelik, G., & Tayfun, U. (2021). Flame retardant effect of boron compounds in polymeric materials. *Composite Part B: Engineering*, *222*, 109088.

[7] Riyazuddin, Rao T. N., Hussain, I., & Koo, B. H. (2020). Effect of aluminum tri-hydroxide/zinc borate and aluminum tri-hydroxide/melamine flame retardant systems synergies on epoxy resin. *Materials Today: Proceedings*, *27*(3), 2269-2272.

[8] Ramazani, S. A, A., Rahimi, A., Frounchi, M., & Radman, S. (2008). Investigation of flame retardancy and physical mechanical properties of zinc borate and aluminum hydroxide propylene composites. *Materials and Design*, *29*(5), 1051-1056.

[9] Carpentier, F., Bourbigot, S., Le Bras, M., & Delobel, R. (2000). Rheological investigations in fire retardancy: Application to ethylene-vinyl-acetate copolymer-magnesium hydroxide/zinc borate formulations. *Polymer International*, *49*, 1216-1221.

[10] Basfar, A. A. (2003). Effect of various combinations of flame-retardant fillers on flammability of radiation cross-linked poly(vinyl chloride) (PVC). *Polymer Degradation and Stability*, *82*, 333-340.

[11] Pi, H., Guo, S., & Ning, Y. (2003). Mechanochemical improvement of the flame retardant and mechanical properties of zinc borate and zinc borate-aluminum trihydrate filled poly(vinyl chlolride). *Journal of Applied Polymer Science*, *89*, 753-762.

[12] Sanchez-Olivares, G., Sanchez-Solis, A., Calderas, F., Medina-Torres, L., Herera-Valencia, E. E., Castro-Aranda, J. I., ... & Alongi, J. (2013). Flame retardant high density polyethylene optimized by on-line ultrasound extrusion. *Polymer Degradation and Stability*, *98*(11), 2153-2160.

[13] Ye, L., Miao, Y., Yan, H., Li, Z., Zhou, Y., Liu, J., & Liu, H. (2013). The synergistic effects of boroxo siloxanes with magnesium hydroxide in halogen free flame retardant EVA/MH blends. *Polymer Degradation and Stability*, *98*(4), 868-874.

[14] Sain, M., Park, S. H., Suhara, F., & Law, S. (2004). Flame retardant and mechanical properties of natural fibre-PP composites containing magnesium hydroxide. *Polymer Degradation and Stability*, *83*, 363-367.

[15] Hollingbery, L. A., & Hull, T. R. (2010). The thermal decomposition of huntite and hydromagnesite-A review. *Thermochimica Acta*, *509*(1), 1-11.

[16] Hollingbery, L. A., & Hull, T. R. (2010). The fire retardant behaviour of huntite and hydromagnesite -A review. *Polymer Degradation and Stability*, *95*(12), 2213-2225.

[17] Hull, T. R., Witkowski, A., & Hollingbery, L. A. (2011). Fire retardant action of mineral fillers. *Polymer Degradation and Stability*, *96*(8), 1462-1469.

[18] Savas, L. A., Deniz, T. K., Tayfun, U., & Dogan, M. (2017). Effect of microcapsulated red phosphorus on flame retardant, thermal and mechanical properties of thermoplastic polyurethane composites filled with huntite & hydromagnesite mineral. *Polymer Degradation and Stability*, *135*, 121-129.

[19] Guler, T., Tayfun, U., Bayramlı, E., & Dogan, M. (2017). Effect of expandable graphite on flame retardant, thermal and mechanical properties of thermoplastic polyurethane composites filled with huntite & hydromagnesite mineral. *Thermochimica Acta*, *647*, 70-80.

[20] Dike, A. S., Tayfun, U., & Dogan, M. (2017). Influence of zinc borate on flame retardant and thermal properties of polyurethane elastomer composites containing huntite-hydromagnesite mineral. *Fire and Materials*, *41*, 890-897.

[21] Ustaömer, D., & Baser, U. E. (2020). Thermal and fire properties of medium-density fiber board prepared with huntite/hydromagnesite and zinc borate. *Biosources*, *15*, 5940-5950.

[22] Atay, H. Y., & Celik, E. (2016). Flame retardant properties of boric acid and antimony oxide accompanying with huntite and hydromagnesite in the polymer composites. *Polymers & Polymer Composites*, *24*, 419-428.

[23] Toure, B., Lopez-Cuesta, J. M., Gaudon, P., Benhassaine, A., & Crespy, A. (1996). Fire resistance and mechanical properties of a huntite/hydromagnesite/antimony trioxide/decabromodiphenyl oxide filled PP-PE copolymer. *Polymer Degradation and Stability*, *53*, 371-379.

[24] Yurddaskal, M., Nil, M., Ozturk, Y., & Celik, E. (2018). Synergetic effect of antimony trioxide on the flame retardant and mechanical properties of polymer composites for consumer electronics applications. *Journal of Materials Science: Materials in Electronics*, *29*, 4557-4563.

[25] Erdem, A., & Dogan, M. (2020). Production and characterization of green flame retardant poly(lactic acid) composites. *Journal of Polymers and the Environment*, *28*, 2837-2850.

[26] Unlu, S. M., Dogan, S. D., & Dogan, M. (2014). Comparative study of boron compounds and aluminum trihydroxide as flame retardant additives in epoxy resin. *Polymer Advanced Technologies*, *25*, 769-776.

[27] Terzi, E., Kartal, S. N., Piskin, S, Stark, N., Figen, A. K., & White, R. H. (2018). Colemanite: A fire retardant candidate for wood plastic composites. *Bioresources*, *13*, 1491-1509.

[28] Ostman, B. A. L. (1984). Fire retardant wood fiber insulating board. *Journal of Fire Sciences*, *2*, 454-467.

[29] Terzi, E. (2018). Thermal degradation of particle boards incorporated with colemanite and common boron based fire retardants. *Bioresources*, *13*, 4239-4251.

[30] Zhong, J., Cui, Y., Zhu, J., & Wang, H. (2016). Preparation and application of colemanite matrix complex flame retardant. *Materials Science Forum*, *852*, 670-676.

[31] Kaynak, C., & Isıtman, N. A. (2011). Synergistic fire retardancy of colemanite, a natural hydrated calcium borate, in high-impact polystyrene containing bominated epoxy and antimony oxide. *Polymer Degradation and Stability*, *96*, 798-807.

[32] Atikler, U., Demir, H., Tokatlı, F., Tıhmınlıoglu, F., Balkose, D., & Ulku, S. (2006). Optimisation of the effect of colemanite as a new synergistic agent in an intumescent system. *Polymer Degradation and Stability*, *91*, 1563-1570.

[33] Cavodeau, F., Viretto, A., Otazaghine, B., Lopez Cuesta, J. M., & Delaite, C. (2017). Influence of colemanite on the fire retardancy of ethylene-vinyl acetate and ethlene-methyl acrylate copolymers. *Polymer Degradation and Stability*, *144*, 401-410.

[34] Isıtman, N. A., & Kaynak, C. (2012). Effect of partial substitution of aluminum hydroxide with colemanite in fire retarded low density polyethylene. *Journal of Fire Sciences*, 31, 73-84.

[35] Borazan, A. A., & Gokdai, D. (2018). Pine cone and boron compounds effect as reinforcement on mechanical and flammability properties of polyester composites. *Open Chemistry*, *16*, 427-436.

[36] Polat, O., & Kaynak, C. (2016). Use of boron oxide and boric acid to improve flame retardancy of an organophosphorus compound in neat and fiber reinforced polyamide-6. *Journal of Vinyl Additive Technology*, *22*, 300-310.

[37] Tang, S., Qian, L., Qiu, Y., & Dong, Y. (2018). Synergistic flame retardant effect and mechanisms of boron/phosphorus compounds on epoxy resins. *Polymers for Advanced Technologies*, *29*, 641-648.

[38] Ibibikcan, E., & Kaynak, C. (2014). Usability of three boron compounds for enhancement of flame retardancy in polyethylene-based cable insulation materials. *Journal of Fire Sciences*, *32*, 99-120.

[39] Frost, R. L., Scholz, R., Ruan, X., & Lima, R. (2016). Thermal Analysis and infrared emission spectroscopy of the borate mineral colemanite (CaB3O4(OH)3.H2O). *Journal of Thermal Analysis and Calorimetry*, *124*, 131-135.

[40] Zarenezhad, B. (2003). Production of crystalline boric acid through the reaction of colemanite particles with propionic acid. *Developments in Chemical Engineering and Mineral Processing*, *11*, 363-380.

[41] Alkan, M., & Dogan, M. (2004). Dissolution kinetics of colemanite in oxalic acid solutions. *Chemical Engineering and Processing: Process Intensification*, *43*, 867-872.

[42] Kopinke, F. D., Remmler, M., Mackenzie, K., Möder, M., & Wachsen, O. (1996). Thermal decomposition of biodegradable polyesters-II. Poly(lactic acid). *Polymer Degradation and Stability*, *53*(3), 329-342.

[43] Westphal, C., Perrot, C., & Karlsson, S. (2001). Py-GC/MS as a means to predict degree of degradation by giving microstructural changes modelled on LDPE and PLA. *Polymer Degradation and Stability*, *73*, 281-287.

[44] Balachander, L., Ramadevudu, G., Shareefuddin, M., Sayanna, R., & Venudhar, Y. C. (2013). IR analysis of borate glases containing three alkali oxides. *Science Asia*, *39*, 278-283.

[45] Wang, M., Wu, Y., Li, Y.D., & Zeng, J. B. (2017). Progress in toughening poly (lactic acid) with renewable polymers. *Polymer Reviews*, *57*, 557-593.

[46] Krishnan, S., Pandey, P., Mohanty, S., & Nayak, S. K. (2016). Toughening of poly lactic acid: an overview of research progress. *Polymer Plastics Technology and Engineering*, *55*, 1623-1652.

[47] Mekonnen, T., Mussone, P., Khalil, H., & Bressler, D. (2013). Progress in bio-based plastics and plasticizing modifications. *Journal of Materials Chemistry A*, *1*, 13379-13398.

[48] Qian, Y., Zhou, S., & Chen, X. (2017). Flammability and thermal degradation behavior of vinyl acetate/layered double hydroxides/zinc borate composites. *Polymers for Advanced Technologies*, *28*, 353-361.